sustainability

MDPI

Article

Understanding Tsunami Evacuation via a Social Force Model While Considering Stress Levels Using Agent-Based Modelling

Constanza Flores [1,2,3,*,†,‡], Han Soo Lee [1,4] and Erick Mas [5]

[1] Transdisciplinary Science and Engineering Program, Graduate School of Advanced Science and Engineering, Hiroshima University, 1-5-1 Kagamiyama, Higashi-Hiroshima 739-8529, Japan; leehs@hiroshima-u.ac.jp
[2] Department of Civil and Natural Resources Engineering, University of Canterbury, Christchurch 8140, New Zealand
[3] School of Engineering, RMIT University, Melbourne, VIC 3000, Australia
[4] Center for the Planetary Health and Innovation Science (PHIS), The IDEC Institute, Hiroshima University, 1-5-1 Kagamiyama, Higashi-Hiroshima 739-8529, Japan
[5] International Research Institute of Disaster Science, Tohoku University, Sendai 980-8572, Japan; mas@tohoku.ac.jp
* Correspondence: constanzaf.henriquez@gmail.com
† Second affiliation is current main affiliation.
‡ Third affiliation is current secondary affiliation.

Abstract: Given massive events, such as demonstrations in coastal cities exposed to tsunamigenic earthquakes, it is essential to explore pedestrian motion methods to help at-risk coastal communities and stakeholders understand the current issues they face to enhance disaster preparedness. This research targets SDG 11 Sustainable Cities and Communities. It strengthens resilience in coastal areas by implementing a social force model using a microscopic agent-based model to assess the impact of human behaviour on evacuation performance by introducing evacuation stress levels due to a tsunami triggered in central Chile. Two scenarios with two environments and three crowd sizes are implemented in NetLogo. In Scenario 1, pedestrians walk at a relaxed velocity. In Scenario 2, tsunami evacuation stress is incorporated, resulting in pedestrians walking at a running velocity, taking, on average, four times less time to evacuate. We explored more realistic settings by considering the internal susceptibility of each agent to spread tsunami evacuation stress among other evacuees. Results from Scenario 2 show that internal susceptibility effects almost double the mean evacuation time for 200 agents. Findings suggest a trade-off between realism and the minimization of evacuation time. This research is considered a first step toward including stress in tsunami evacuations for sustainable evacuation planning.

Keywords: sustainable evacuation planning; disaster preparedness; tsunami evacuation; coastal resilience; evacuation stress; agent-based modelling

Citation: Flores, C.; Lee, H.S.; Mas, E. Understanding Tsunami Evacuation via a Social Force Model While Considering Stress Levels Using Agent-Based Modelling. *Sustainability* **2024**, *16*, 4307. https://doi.org/10.3390/su16104307

Academic Editor: Xuelong Li

Received: 5 April 2024
Revised: 26 April 2024
Accepted: 15 May 2024
Published: 20 May 2024

1. Introduction

Events such as celebrations, sports competitions, pilgrimages, and demonstrations are examples of massive gatherings where thousands of people unite simultaneously in a specific location. For instance, on 27 October 2019, an extensive march gathered 100,000 people in the streets of Valparaiso City, central Chile [1]. A similar number of people—approximately 80,000—gathered in the Itaewon district of Seoul, South Korea, on 29 October 2022 during Halloween celebrations, but with fatal consequences [2]. Evacuations caused by false bomb alarms [3], car attacks [3], fires [4], or disasters such as earthquakes [5,6] or tsunamis [7] can rapidly raise people's stress levels, triggering a variety of behavioural responses. In emergencies, for instance, stressed individuals walk faster during evacuations than they do under non-evacuation scenarios [3,8,9].

To prevent crowd disasters, such as the one that occurred in the Itaewon district [2], where more than 150 casualties were reported because of crowd surges due to extremely

high densities in narrow streets, it is essential to understand the dynamics and emergent phenomena behind heterogeneous crowds. There is significant uncertainty about human behaviour in life-threatening situations, especially under stress.

Agent-based models (ABMs) are powerful and flexible tools used in diverse disciplines, from natural and social sciences to engineering [10]. The tsunami evacuation field is not an exception; ABMs are suitable for studying pedestrian evacuation modelling due to their ability to simulate the emergent phenomena resulting from agent–agent and agent–environment interactions [7,11–13]. For instance, the comprehensive multimodal ABM work of [7] addresses the controversial topic of vehicle usage in tsunami evacuations in Kamakura, Japan. In their simulations, the consideration of the behaviours and the degree of interactions of residents and visitors with the urban settings is of great importance for disaster preparedness in touristic cities. After the Great East Japan Earthquake (GEJE) in 2011, the authors of [11] modelled a village-wide multimodal evacuation using the ABM NetLogo. With a geographically explicit model that includes building layouts, road networks, tsunami safe zones, and shelters, they examined several behaviours related to the GEJE tsunami. The simulations considered shelter capacity, casualty estimation, traffic jam location, and a collision avoidance algorithm for pedestrian motion and subsequent interaction.

The social force model (SFM) is a continuous microscopic approach utilized to represent pedestrian motion under the concepts of driving, interacting, and physical forces. These forces enable evacuees to move toward a destination, help them avoid collisions with other evacuees while maintaining their private space, and prevent them from colliding with environmental features, such as walls or obstacles [14]. The SFM can realistically reproduce pedestrian movement in normal and emergency contexts [14–16]. The implementation of a pedestrian motion approach capable of realistically representing individual evacuees' movement (SFM) in a platform (ABM) where interactions between evacuees and the environment can be analyzed at the individual level is a reasonable method for the numerical modelling of human behaviour in the context of a tsunami evacuation event. According to the extensive pedestrian evacuation ABM review of [17] that covered eighty-one research papers over a period of ten years, in building and outdoor evacuations—regardless of the type of hazard (e.g., floods or tsunamis)—human behaviour is the main topic of study, meaning that this technique is a reliable and extensively used tool for emergency evacuation simulations.

2. Literature Review

Socio-psychological aspects in evacuations have been studied for various emergency situations [3–6]. However, few are dedicated to the tsunami hazard and its consequent evacuation process. A multiagent-based model employing a microsimulation based on the SFM was used on French Riviera beaches to study tsunami evacuation behaviour [18]. Another study combined an agent-based simulation (ABS) with a Susceptible-Exposed-Infectious-Recovered (SEIR) model to analyze the COVID-19 spread in a tsunami evacuation in Iquique, Chile [19]. Susceptible, exposed, infectious, and recovered agents with different contagion rules based on probability functions were modelled in this study. An ABS for a city-wide tsunami evacuation, including a simplified SFM, was utilized in the two Chilean cities of Iquique and Viña del Mar, as well as in Kesennuma, Japan [20]. Similarly, in Viña del Mar [21,22] and Valparaiso [22], city-wide and drill-wide tsunami evacuation simulations incorporated a collision avoidance algorithm into an ABM. León and March [23] analyzed the impact of urban features on evacuation times in the tsunami-exposed city of Talcahuano in Chile, via an ABM. In the authors' preliminary work [24], to represent pedestrian motion in tsunami settings, initial values for the parameters of the SFM are tested. Using the ABM NetLogo, pedestrian evacuees walking both at a relaxed velocity and evacuating at high velocities are simulated. Additionally, a preliminary proposal to estimate stress levels is introduced.

Indoor and semi-open investigations covering quantitative methods to estimate emotion contagion and stress variations in evacuation settings have highlighted the need to

include such variables in computer models, seeking to simulate more realistic situations. For instance, Cornes et al. [3] developed a method for spreading fear in crowds, which was inspired by real-life dangerous situations captured on video. They combined the SFM and a Susceptible-Infected-Recovered-Susceptible (SIRS) model to simulate emotional contagion from nearby pedestrians, considering contagion efficiency and internal stress fluctuations. In the context of fire evacuations, Cao et al. [4] studied stress variation in a building evacuation through the SFM. They utilized a sigmoid function to estimate evacuees' stress level based on the distance from the fire source. The earthquake evacuation research of [6] developed a group emotion contagion model based on the OCEAN (Openness, Conscientiousness, Extraversion, Agreeableness, Neuroticism) personality model, considering leadership effect, agent–environment interaction, and pedestrian motion planning. Also being in the earthquake-related field of research, the ABM work of [5] carried out by means of a modified version of the BDI (Belief, Desired, Intentions) approach, proposed a procedure to model anxiety based on perceptions. Agents make decisions based on the perception of the estimated evacuation time, crowd density, and visibility of exits via exponential functions. The evacuation process considered structural and non-structural damage to buildings.

Except for [24], none of these studies have incorporated stress levels in tsunami evacuations utilising a microscopic pedestrian motion approach, for instance, the social force model in a platform capable of simulating interactions at an individual level, such as agent-based modelling. This research aims to fill this gap by investigating human behaviour in a hypothetical near-field tsunami evacuation in Valparaiso City, central Chile, while incorporating stress levels using the NetLogo 6.3.0 software (Figure 1b). The present research is regarded as an initial step in integrating stress variables into numerical modelling within the context of tsunami evacuations. From a risk reduction point of view, the more we understand the complexities of human behaviour in tsunami evacuations, the better we can prepare for future scenarios. Despite the lack of real-world data, hypothesizing behavioural features such as stress in computer simulations can help decision-makers more quickly understand the challenges ahead and the measures required to improve the effectiveness of the current evacuation plans, paving the way to sustainable evacuation strategies.

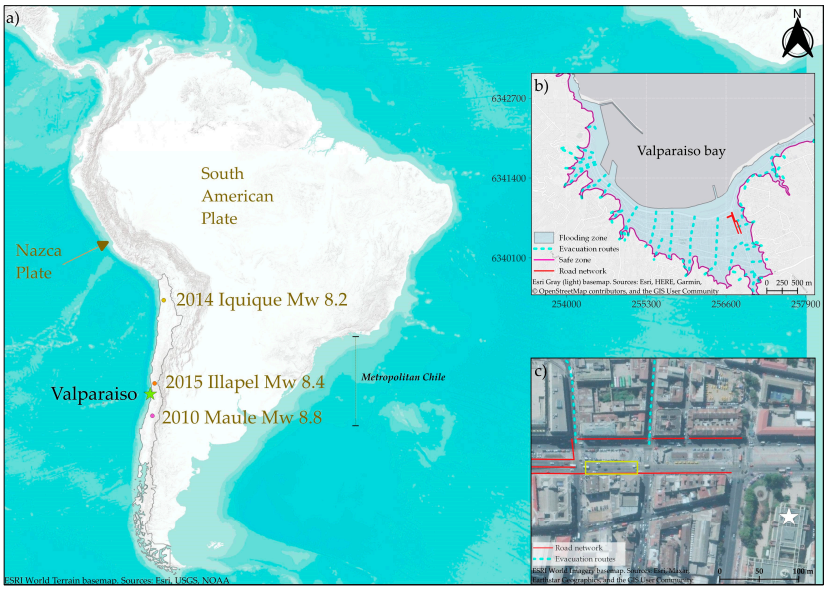

Figure 1. (**a**) Latest earthquakes in Chile. (**b**) Valparaiso city layout including tsunami inundation extent, evacuation routes, and safe zone. (**c**) The study area is shown in yellow, red lines are road networks, and cyan dashed lines indicate evacuation routes. White star is the march destination. Map created with QGIS 3.28.2.

The remaining sections are organized as follows. In Section 3, the materials and methods used, including the Social Force Model, experimental scenarios, tsunami evacuation stress estimation and spread, parameter setting, and NetLogo interface, are explained in detail. In Section 4, the results for the different scenarios are presented. Section 5 outlines the discussion, and conclusions are drawn in Section 6.

3. Materials and Methods

3.1. Study Area

Chile is one of the most tectonically active areas in the world due to the convergence zone between the Nazca and South American plates which lies underneath it [25]. Earthquakes with magnitudes greater than Mw 8 occur once every 10 years [26]. Over the recent 14 years, the country has witnessed three major earthquakes that triggered tsunamis (Figure 1a): the Maule earthquake on 27 February 2010 of magnitude Mw 8.8, the Iquique earthquake on 1 April 2014 of magnitude Mw 8.2, and the Coquimbo earthquake on 16 September in 2015 (Mw 8.4) [27]. According to Carvajal et al. [28], in 1730, an earthquake of Mw 9.1–9.3 struck Metropolitan Chile (see Figure 1c). Since that time, neither of the latest earthquakes of 1822, 1906, and 1985 have liberated most of the shallow slip accumulated in the area. Future tsunamis have great potential to be destructive, posing a significant risk for the coastal communities in Metropolitan Chile, where Valparaiso City is located (Figure 1b).

The study area, shown in yellow in Figure 1c, is a section of Argentina Avenue in Valparaiso City. This is the main perpendicular street with respect to the shoreline where people gathered and walked toward the march destination (white star in Figure 1c) on 27 October 2019. The crowd, with a length of approximately 7 km, was composed mainly of families and friends. The concept of a crowd is still challenging to define because of its diversity in terms of sizes and types, i.e., physical or psychological crowds, to name a few [29]. According to [30], a proper definition of a crowd would be a group of "*20 people standing in close proximity at a specific location to observe a specific event over a one-hour period, who feel united by a common identity and, despite being strangers, are able to act in a socially coherent way*".

3.2. Social Force Model

The social force model (SFM) is a microscopic continuous physics-based approach proposed by Helbing and Molnár in 1995 [14]. In this pioneering work, they introduced the study of pedestrian movement via social interactive and driven forces. The driving force (goal force) directs pedestrians to their destination or goal. To ensure a degree of comfort, interactive forces between pedestrians and their surroundings (e.g., walls or obstacles) are repulsive in nature, permitting individuals to maintain their private space while moving to their intended destination. Additionally, attractive forces are incorporated into the model to account for the effect of approaching friends or objects of interest. To consider situations occurring beyond the agents' field of view, for instance, backwards, weights with mild effects are introduced, depending on the deviations from the desired direction. Lastly, this version of the SFM considers fluctuations because of random or unpredictable behaviours.

In Helbing et al.'s [8] following work in 2000, which aimed to quantitatively study high-density panicking situations, a crowd scenario was introduced. Values were presented for the key parameters for the repulsive interactive forces, named strength (A_i, A_{iw}) and reach (B_i, B_{iw}). Physical forces that are relevant in high-density scenarios, both normal and tangential, were also described, along with their respective parameters. These physical interactive forces help evaluate potential injuries in emergencies or unsafe situations, which is out of the scope of the present study.

$$\frac{dv_i}{dt} = f_{des} + \sum_{j=1}^{N} f_{ij} + \sum_{j=1}^{N} f_g \quad (1)$$

In the context of escape panics, according to Helbing et al. [8], Newton's motion equations are utilized to represent velocity variations of N pedestrians over time (dv_i/dt) by taking into account one driving and two interactive repulsive forces—the desired force (f_{des}), the social force (f_{ij}), and the granular force (f_g)—as shown in Equation (1). The latter force represents physical contact at high densities where body force and sliding friction emerge either because of the interactions between pedestrians or a pedestrian and walls/objects.

$$f_{des} = \frac{v^i_{des}(t)e^i_{des}(t) - v^i(t)}{\tau} \quad (2)$$

In Equation (2), the driving force (f_{des}) accounts for any pedestrian i navigating toward a goal (e.g., safe zone or evacuation shelter) in a desired direction ($e^i_{des}(t)$) at a desired velocity ($v^i_{des}(t)$). Deceleration due to interactions with the environment and other individuals triggers deviations from the desired velocity, causing agents to instead move at a current velocity ($v^i(t)$). As pedestrians strive at every time step to attain their desired velocity, the concept of relaxation time (τ) is incorporated to represent agents' behaviour. Small values for τ result in individuals walking more aggressively [14].

$$f_{ij} = f_{sij} + f_{bij} = A_i\, e^{(rij-dij)/Bi}\, n_{ij} + k_n\, g(r_{ij} - d_{ij})\, n_{ij} \quad (3)$$

Interactions between pedestrians and interactions of pedestrians with walls or objects are taken into consideration by the socio-psychological force or social force (f_{ij}) in Equation (3). The social force equation for interactions between pedestrians considers socio-psychological (f_{sij}) and physical or contact forces (f_{bij}). Once in motion, individuals desire to preserve a minimum distance from others, walls, or objects. Figure 2 shows a schematic representation of two interacting agents, in which the pedestrian radius (r_i, r_j) symbolises the personal or private space. Interactions, which are repulsive in nature, are ruled by an exponential function decay with two constant values, A_i strength of social interaction and B_i reach of social interaction. If the length of the distance separating pedestrian i and pedestrian j's centre of mass is greater than the sum of the pedestrian's radius ($d_{ij} > r_{ij}$), agents are not in contact; hence, they do not collide (Figure 1). Conversely, if the sum of the pedestrian's radius exceeds the length of the distance between the pedestrian's centre of mass, $r_{ij} > d_{ij}$ agents collide with each other. The collision triggers a physical force f_{bij} with a body force coefficient k_n and a Heaviside function $g(r_{ij} - d_{ij})$ set to zero when there is no contact between agents, or it is set to the argument if collisions occur. Lastly, the unit vector n_{ij} points from pedestrian j to pedestrian i.

$$f_g = f_{siw} + f_{biw} = A_{iw}\, e^{(ri-diw)/Biw}\, n_{iw} + k_n\, g(r_i - d_{iw})\, n_{iw} \quad (4)$$

The social force for interactions between pedestrians and walls or objects is shown in Equation (4). These interactions are also repulsive in nature, and they are ruled by the exponential function decay with constant parameters A_{iw} (strength of the social interaction between pedestrians and walls or objects) and B_{iw} (reach of the social interaction between agents and walls or objects). The term r_i represents the radius of any pedestrian i, d_{iw} is the normal distance from the current agents' position to the wall, and n_{iw} is the unit vector heading its direction from the wall into any given pedestrian i. Similar to Equation (3), if agents make contact with walls, physical forces with a body force coefficient k_n and the corresponding Heaviside function appear. Finally, to account for the interactions between agents and obstacles (f_{si_obs}, f_{bi_obs}), the same Equation (4) is used.

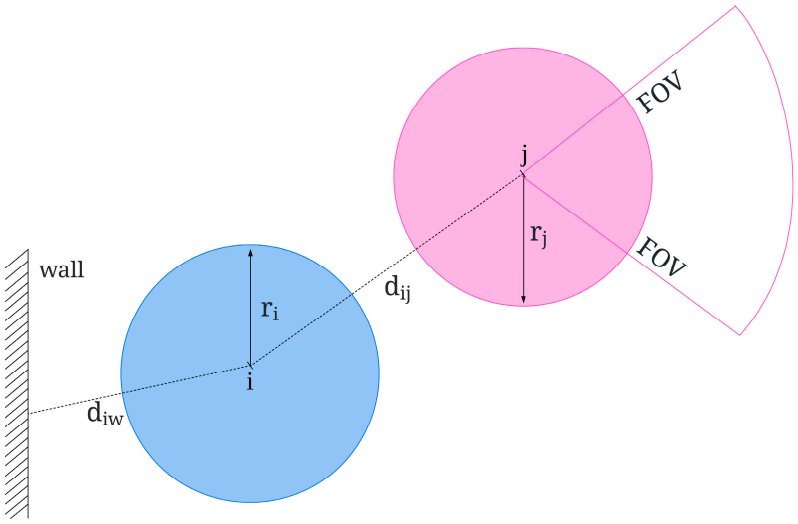

Figure 2. Schematic representation of two interacting agents.

SFM Parameters

Given the absence of empirical data and the use of a hypothetical case, this study adopts a theoretical approach to investigate pedestrian dynamics in a tsunami evacuation event in central Chile, with two experimental scenarios implemented in NetLogo. To represent pedestrian movement more realistically, we applied the SFM and set up the parameters for the interactive and driven forces based on values from the literature, both in the context of emergencies and during normal situations (Table 1).

Table 1. Suggested parameters for the SFM in the literature.

Reference	A_i [m/s^2]	B_i [m]	A_{iw} [m/s^2]	B_{iw} [m]	τ[s]	v^i [m/s]
Helbing et al. [8]	27	0.08	27	0.08	0.5	0.8
Helbing et al. [16]	3	0.2	5	0.1	1	Normal distribution. Mean = 1.3 SD 0.3

In a preliminary work [24], the authors tested the SFM in NetLogo in a unidirectional corridor using the following values from [1]: A_i = 10 N, A_{iw} = 2000 N, B_i = 0.13 m, and B_{iw} = 0.08 m. However, the constant oscillations of agents led to the conclusion that further calibration is necessary to adequately represent pedestrian motion.

In the present research, several experiments were carried out to determine the most suitable set of parameters for the two scenarios (Scenario 1 and Scenario 2). While testing the values in Table 1, oscillations and undesired behaviours (such as pushy behaviour and unrealistic large jumps) emerged from the simulations. To address this issue, sensitivity and trajectory analyses were performed. Research on parameter calibration of the social force model with empirical data indicates that a different parameter combination might produce equivalent outcomes [31–33]. The parameter setting criterion applied in this study was to identify the combination that eliminates oscillations, overlapping, and unrealistic behaviour with a minimum variation from the values in Table 1. We minimised the oscillations as much as possible while avoiding overlapping, which is a well-known dual issue in the SFM [34–36]. The chosen values for the strength and reach of the interactive repulsive force f_{sij} were 3 m/s^2 and 0.2 m, respectively, while for the repulsive forces for walls and obstacles, they were 40 m/s^2 and 0.2 m, respectively (refer to Table 2).

Table 2. Experimental parameters for the SFM.

Parameter		Scenario 1	Scenario 2
Symbol	**Unit**		
A_i	m/s^2	3	
B_i	m	0.2	
A_{iw}, A_{iobs}	m/s^2	40	
B_{iw}, B_{iobs}	m	0.2	
τ	s	1	0.6
v^i	m/s	0.6 + 0.1	1
v_{des}	m/s	0.66	Sigmoid
r_i	m	Normal distribution. Mean = 0.466, SD 0.031	
mass	kg	78.45	
k_n	kg/s^2	1.2×10^5	
FOV_radius	m	3	1
rj_radius	m	3	1
FOV_obs	m	3	1
FOV_walls	m	3	1
k		-	2
spread_radius	m	-	>1

3.3. Experimental Scenarios

The agent-based model (ABM) NetLogo [37] is used to implement the SFM. NetLogo is a robust and flexible open-source ABM widely utilized to model complex systems with a broad range of applications, including the pedestrian evacuation field and tsunami evacuations [10,37]. Several studies have used NetLogo for modelling tsunami evacuations in Japan [11,38], Indonesia [13,38], Peru [39], and Chile [12,24]. NetLogo employs a bottom-up approach to simulate complex systems. Agent-based models are useful for modelling systems or natural phenomena using agents (autonomous adaptive heterogeneous entities), an environment (a computational world where agents move), and agent–agent/agent–environment interactions. One of the key properties of complex systems is emergent phenomena (macro-level aggregated behaviours), which result from the reciprocal interaction between agents and the environment, even when straightforward rules are followed [10].

Figure 3 shows a summary of the model's implementation. After setting up the model by assigning attributes to the agents and producing the environments, two scenarios were executed. Scenario 1 depicts the protest with agents walking on Valparaiso's city street at an easy pace. Scenario 2 is a hypothetical tsunami evacuation event that includes tsunami evacuation stress. In the simulations, crowd sizes of 50, 100, and 200 agents were examined. Evacuation time varies depending on the number of agents and environment settings, but the maximum mean evacuation time considering all agents evacuated for the largest crowd is ~130 s (check Table 3). The effect of obstacles on the mean evacuation time is also investigated, and both scenarios are compared. Results are shown in Section 4, including the outcomes of the tsunami evacuation stress spread for low, intermediate, and high susceptibility levels.

Table 3. Mean evacuation times for 50, 100, and 200 agents in two different environments in Scenario 1.

Agents	No Obstacles	Obstacles	Difference
50	92.70	98.53	6.29%
100	103.67	108.67	4.82%
200	123.33	129.23	4.78%

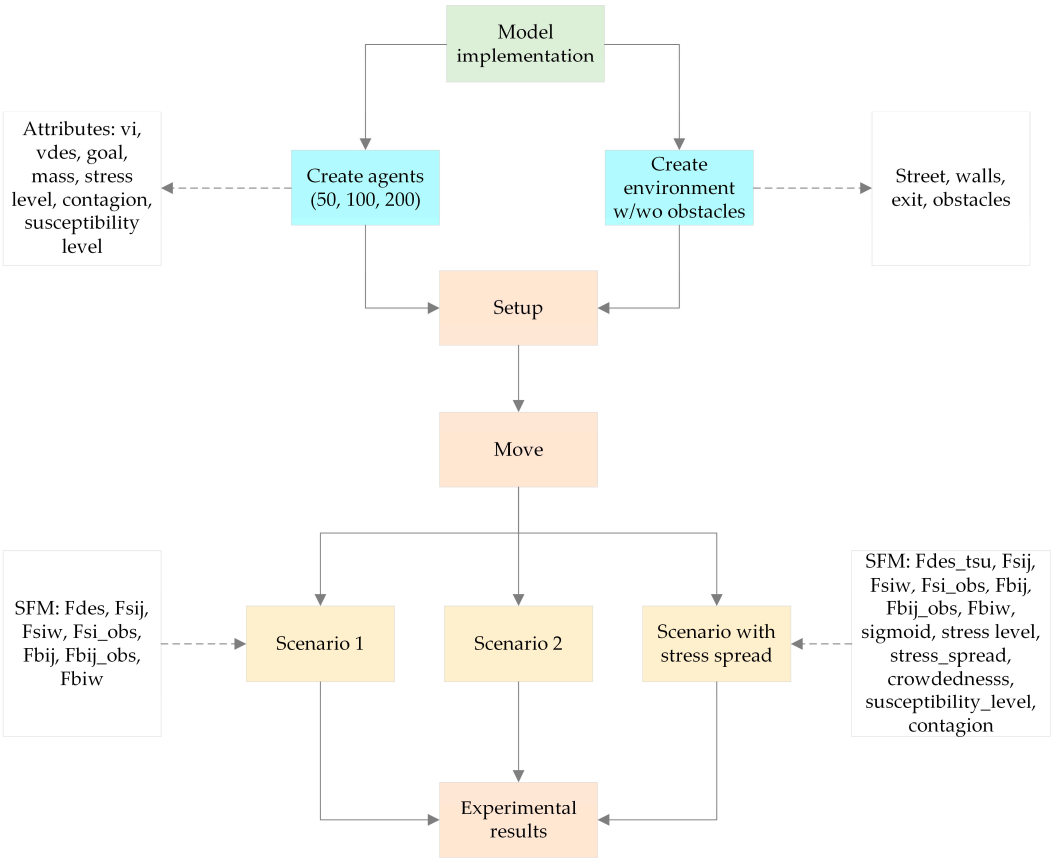

Figure 3. NetLogo implementation flowchart.

3.4. Tsunami Evacuation Stress and Spread

Recent studies investigating quantitative approaches to estimate stress fluctuations in indoor and semi-open emergency evacuations have utilized sigmoid [4] and exponential decay functions [3,5]. Behavioural changes in evacuees' moving velocities due to stress variations are discussed in the context of the SFM in references [3,4]. In the authors' previous work [24], a similar method was proposed to calculate tsunami evacuation stress, in which velocity alterations because of escalating stress were accounted for by the desired force (Equation (2)). It is well established that people move faster in emergencies or life-threatening circumstances than in ordinary situations. Therefore, their desired velocities exceed those in non-emergency situations (e.g., Scenario 2 vs. Scenario 1). Then, according to [24], a sigmoid function fluctuating in the range [0, 1], in which 1 symbolizes the maximum tsunami stress level and 0 the minimum tsunami stress level, was proposed (Equation (5)). Stress varies based on the distance ($d_i^{exit}(t)$) to the safe zone, where the farther the distance from the agents' actual position to the safe zone, the higher the stress. The closer they are to the safe zone, the lower the stress. Lastly, k is the slope of the sigmoid function (see Table 2).

$$S_i^t = \frac{1}{1+e^{(-k \times d_i^{exit}(t))}} \quad (5)$$

In our preliminary work [24], the piecewise function was modified from Cao et al. [4], with velocity values as follows to account for the variations in the desired velocity because of tsunami evacuation stress. For the high stress level, the value of 5 m/s came from [8]. We referred to [4] for intermediate stress, while the low stress level value of 0.66 m/s was obtained from secondary data. The desired velocity is modified and adapted to a tsunami context in the present research, as shown in Equation (6). Agents in the high stress level have a maximum speed of 2.77 m/s, which is the mean of the low, moderate,

and fast running speeds from Wood et al. [40]. The results of Fraser et al. [41], after studying the probability of pedestrians running at slow, moderate, and fast speeds in a least-cost tsunami evacuation model, emphasize the positive effect in the evacuation time of integrating evacuees moving at running speeds in computer simulations. In the present study, the decision to select running speed values is to minimise the evacuation time in a tsunami scenario and to simulate a high-stress situation caused by a near-field tsunami with less than 15 min before the arrival of the first wave. Mild-stress velocity is determined from secondary data from [24] (further details in Section 3.5 and Table 2), including a randomness of 0.34 m/s to resemble agents walking faster than in relaxing settings. The intermediate stress value for the desired velocity corresponds to the linear equation between the mild and high stress levels.

$$v_d^i(t) = \begin{cases} 2.77 & high\ stress\ if\ S_i^t \geq 0.9 \\ 2.2125 \times S_i^t + 0.77875 & intermediate\ stress\ if\ 0.9 > S_i^t \geq 0.1 \\ 1 & mild\ stress\ if\ S_i^t < 0.1 \end{cases} \quad (6)$$

One of the limitations of this approach is that stress drops in the vicinity of the exit. For most of the simulation time, agents navigate the environment at a high stress level, resembling a running crowd. Evacuees with similar distances to the safe zone have the same stress level. Hence, stress variations among the crowd are low. A valid question is how realistic this approach is, especially considering that stress levels could vary between individuals in a real tsunami event. To explore more real-life settings, further experiments are executed to clarify the impact of the spread of stress on the total mean evacuation time. Each agent's tsunami evacuation stress spread is linked to its internal susceptibility level. At the beginning of the simulation, every agent is randomly assigned one of the three proposed susceptibility levels: high, intermediate, and low. The resulting number of agents in each of the levels is approximately proportional to 70, 63, and 67 for 200 agents, representing the worst condition in terms of crowdedness.

Drawing from the fear propagation method of [3], in which a contagion efficiency-based formulation is introduced to spread emotions among individuals in crowding contexts, the efficiency of spreading is a function of the effective contagion stress and the proportion of individuals in fear state within a certain radius. In this research, a new stress variation method is proposed using a simpler approach adapted to a tsunami context. Based on the contagion rate C, individuals shift their stress level from intermediate to high, defined as the ratio of neighbours in high stress over the total number of neighbours in a given spread radius, as shown in Equation (7) and Figure 4. Since the settings of this scenario comprise a near-field tsunami evacuation event with a short evacuation time, mild stress is not taken into consideration.

$$C = \frac{\text{number of agents in high stress}}{number\ of\ neighbors} \quad (7)$$

Various researchers have investigated the tendency of individuals to imitate other people's actions during evacuations. Often, individuals follow their neighbours' lead rather than making decisions themselves, which is a form of social influence [42]. In this research, agents with a high level of susceptibility mimic others easily, leading to the transition from an intermediate stress level to a high level. This transition happens if C > 0, signifying that the presence of even a single neighbour (within the spread radius) under high stress can trigger a change in their current stress level. In the simulations, agents compute their contagion rate at every time step. Those with medium susceptibility shift their stress level if C > 0.5. Lastly, agents with low susceptibility are less likely to mimic others; to alter their current level of stress they require all neighbours to be under high stress (C = 1).

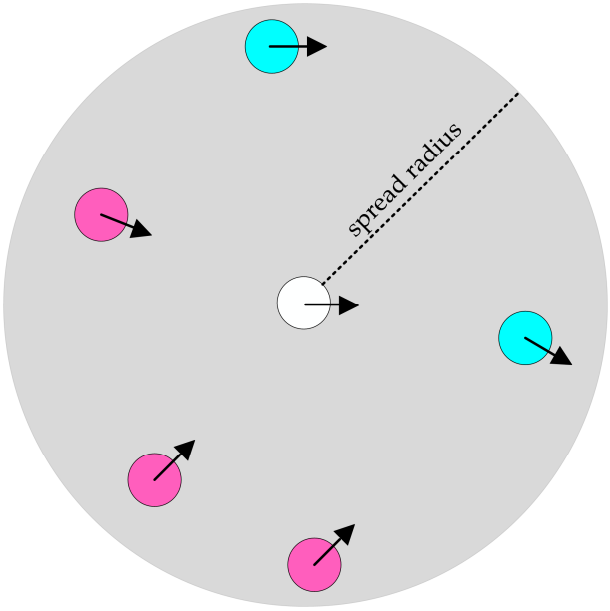

Figure 4. Tsunami stress spread. The white agent represents any other agent assessing its contagion rate C at every time step for the given spread radius. Cyan colour depicts agents subjected to intermediate stress while magenta indicates agents subjected to high-stress.

3.5. Model Parameter Setting

In this section, the parameters selected for each of the experimental scenarios are explained and listed in Table 2. As mentioned in Section 3.2, the relaxation time represents the reactiveness with which pedestrians correct variations from their instantaneous velocity in relation to the desired one. The lower this value is, the more aggressive the agent is when reacting to deviations [8,14]. For Scenario 1 (no tsunami), the decision to choose $\tau = 1$ s is to resemble pedestrians walking at a relaxed velocity; hence, choosing a higher relaxation time will make pedestrians react in a more relaxed fashion. In contrast, for Scenario 2 (tsunami), a lower value is considered appropriate for an evacuation context including stress. $\tau = 0.6$ s in Table 2 slightly varies from that of Helbing et al. [8] due to better performance in sensitivity analysis. The variation from the suggested value is 20%, as oscillations increase significantly when $\tau = 0.5$ s.

The value for the actual/instantaneous velocity for Scenario 1 is obtained from [24], with a randomness of 0.1 m/s being added to it. According to [24], drone footage that was recorded for 4 min and 1 s captured the demonstration moving between the cities of Viña del Mar and Valparaiso [43]. The recording angle and the continuous drone motion are the footage's limitations for data extraction, posing difficulties to extract densities and velocities manually. It was found that there are only a few records available in a static position. Two video sections that are six seconds in length, starting at 00:49 (mm:ss) and 02:49 (mm:ss) were used to estimate local density and instantaneous velocity. After manually counting people inside the yellow square junction (see [43] at 00:52 (mm:ss)) and following representative pedestrians located at the centre of the square, a density of 1.3 ped/m^2 and a velocity of 0.66 m/s were obtained. Although the data are discrete, and the drone record does not cover Argentina Avenue (yellow area in Figure 1c), the values are regarded as indicative of the entire crowd, which extends to a length of approximately 7 km. To provide a distinct instantaneous velocity value to each agent in the simulation and account for the discontinuous nature of the metrics, a randomness of 0.1 m/s was introduced into the model (Table 2). The desired velocity (v_{des}) for Scenario 1 is equal to the actual velocity (0.66 m/s); for Scenario 2, it is set according to the value of the sigmoid function, as explained in Section 3.4.

To increase heterogeneity in the model, the radius (biacromial breadth/2) of the circular specification used in this study follows a normal distribution with a mean of

0.466 m and a standard deviation of 0.031 m [44]. The mass, fixed at 78.45 kg for all agents in the simulation, is the mean of both female and male Chilean adult workers aged 18–65+ years [44]. The body force coefficient is from Helbing et al. [8]. The field of view (FOV, Figure 2) specifies how in advance agents can inspect features of the environment, such as obstacles (FOV_obs), walls (FOV_walls), or other individuals (FOV_radius, rj_radius) at each time step. Previous studies have used a radius of view of 5 m in their models [11,15,20,45]. Other experiments were performed using a maximum length of view of 10 m [46]. However, some papers considered 5 m to be a sufficiently large distance for interactions in terms of numerical efficiency [47]. For Scenario 1 (no tsunami), the field of view is 3 m because of the computational efficiency. Sensitivity analysis revealed that differences in the field of view did not affect the evacuation time. Tunnel vision may occur during stressful and unsafe situations [48]. To consider this effect in the modelling carried out in this study, the field of view in Scenario 2 (tsunami) equals 1 m. The slope of the sigmoid function is 2 [4]. Finally, as the sensitivity analysis showed, the evacuation time is not sensitive to spread radii between 0.5 m and 3 m, and the spread radius is greater than 1 m.

3.6. NetLogo Model Setup

Figure 5 illustrates the unidirectional corridor with dimensions of 51 × 13 cells and a spatial resolution of 1 m, replicating a section of Argentina Avenue (Figure 1c). Agents are created on the left side (purple vertical line) and navigate the world from left to right until reaching the narrow rectangular exit, which is coloured brown. The walls are lime-coloured (1 m width). Pedestrians in white are circular in shape and denote Chilean adults between 18 and 65+ years old [44]. After postprocessing the SRTM 30 m resolution DEM, it was determined that the slope in the study area is mild (less than 3.5%); therefore, the slope effect is neglected in the simulations.

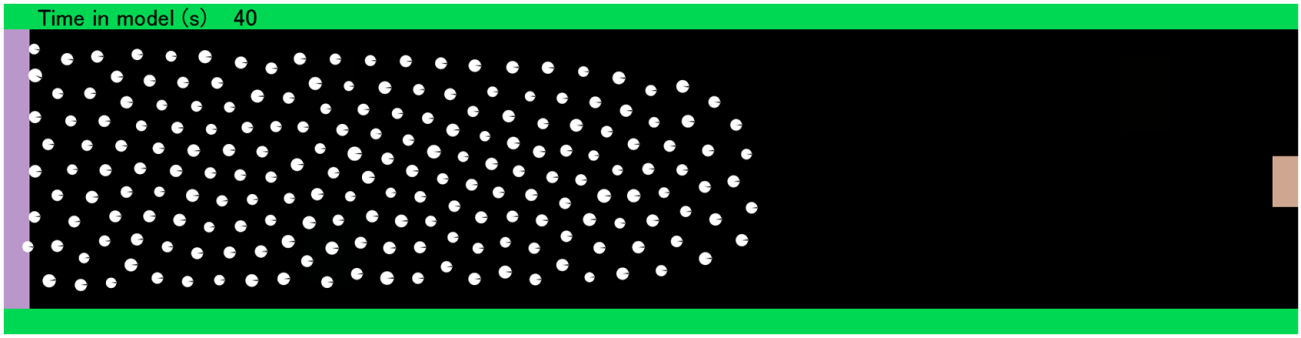

Figure 5. The NetLogo environment with 200 agents in the simulation.

Figure 6 shows the interface and the settings for environments with obstacles. We placed three lines comprising five obstacles each, which are represented by green squares. The upper and lower lines are two cells away from the walls, and the distance between obstacles is seven cells. The central line is in the middle of the street. The criteria used for the settings is to leave enough space to create agents and to let them exit the street. To allow for sufficient interaction between agents and obstacles, we set the obstacles as equidistant as possible within the NetLogo environment. The simulation time step is 0.033 s. The code was modified from Mas et al. [11].

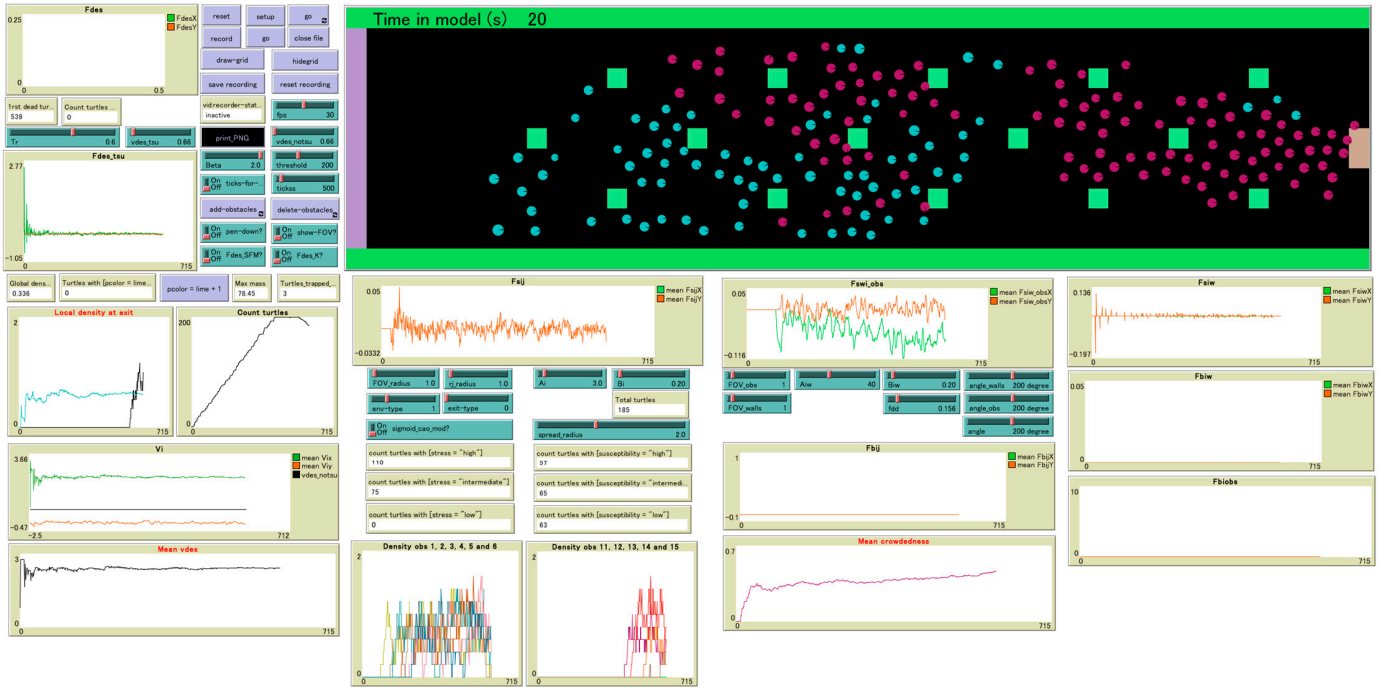

Figure 6. The NetLogo interface includes buttons to setup, start, stop, and reset the simulation. Monitors show the number of agents in the simulation over time (total turtles), time it takes the first agent to reach the safe zone (first evacuee), and changes in the global density over time (global density). Sliders are used for setting each of the parameters of the SFM (A_i, A_{iw}, B_i, B_{iw}, FOV_radius, rj_radius, FOV_obs, FOV_wall) and tsunami stress spread (spread_radius, beta, Tr). Plots are used to monitor the instantaneous velocity (v_i), social interaction, body and driving forces (F_{sij}, F_{siw}, F_{siw_obs}, F_{bij}, F_{biobs}, F_{biw}, F_{des}, F_{des_tsu}), evacuation curve (count turtles), local density at the exit (local density at exit), and local density near obstacles (density obs).

4. Simulation Results

4.1. Mean Evacuation Time: Scenario 1 and Scenario 2

The evacuation time corresponds to the time it takes for all agents to successfully evacuate the environment (exit in brown, see Figure 5). To investigate the effect of diverse environment settings and crowd sizes on the evacuation time, multiple experiments were carried out for Scenario 1 and Scenario 2. Results outline the mean evacuation time for ten runs.

The evacuation curve for crowd sizes of 50, 100, and 200 evacuees for Scenario 1 (no tsunami) is presented in Figure 7. At every time step of 0.033 s, each cell has a 50% probability of creating an agent of size $2r_i$. To avoid overlapping once creating the agents, a separation of 1 m is defined. At the beginning of the simulation, between 0 and 40 s, the positive slope corresponds to the increasing number of agents according to the given probability, every 0.033 s, for each crowd size. Regardless of the presence of obstacles, each curve enters the stationary phase when the threshold—either 50, 100, or 200 agents—is reached. The larger the crowd size, the sharper the evacuation curve. Additionally, a great number of agents reduces the length of the stationary phase, for instance, 60 s for 50 agents, 50 s for 100 agents, and 30 s for 200 agents. This is because 50 agents occupy less area than 200 agents, meaning that the crowd remains in the simulation for a longer duration before the first agent is successfully evacuated, indicating the end of the stationary phase. The curves keep descending until no agents are left in the simulation.

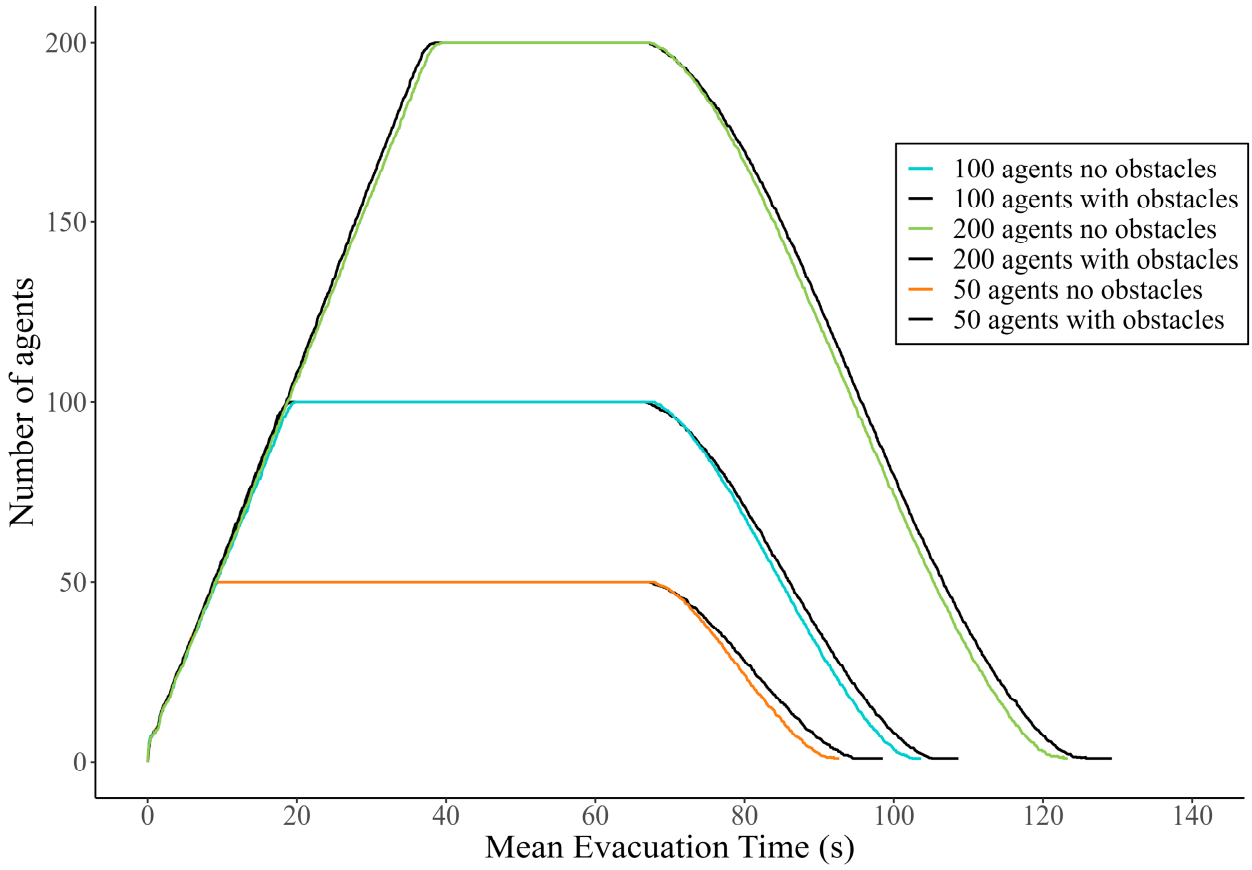

Figure 7. Mean evacuation time curve for 50, 100, and 200 agents in environments with and without obstacles for Scenario 1 (no tsunami).

The longest simulation time, over 120 s, for environments with and without obstacles is for 200 agents, as shown in Table 3. This result is reasonable; the larger the crowd size, the longer the mean evacuation time. The impact on the evacuation time because of the presence of obstacles is mild. When evaluating the mean of the three-group sizes of agents, environments with obstacles take 5.30% longer to evacuate; this difference explains why the coloured lines are parallel to the black lines in Figure 7. Check Table 3 for the details for each crowd size.

Figure 8 presents the mean evacuation time for both scenarios considering environments with and without obstacles. Because of the higher desired velocities in the tsunami scenario, agents take approximately four times less to evacuate, regardless of the existence of obstacles. This scenario follows a similar trend as Scenario 1, in which the larger the crowd, the longer the evacuation time for all of the evacuees. For instance, for settings without obstacles, 200 agents take 30.77 s, 100 agents take 24.40 s, and 50 agents take 21.53 s; refer to Tables 3 and 4 for more details. Cases with obstacles also take longer to evacuate—on average, they take 13.55% longer to evacuate, considering the three crowd sizes. The impact on the mean evacuation time because of obstacles is greater for 100 agents, taking 28.83% more time to evacuate (see Table 4). In contrast, for 200 agents, this impact is only 2%, indicating that obstacles practically do not affect the mean evacuation time. A similar situation occurs for 50 agents, in which the difference in the mean evacuation time due to obstacles is less than 10%.

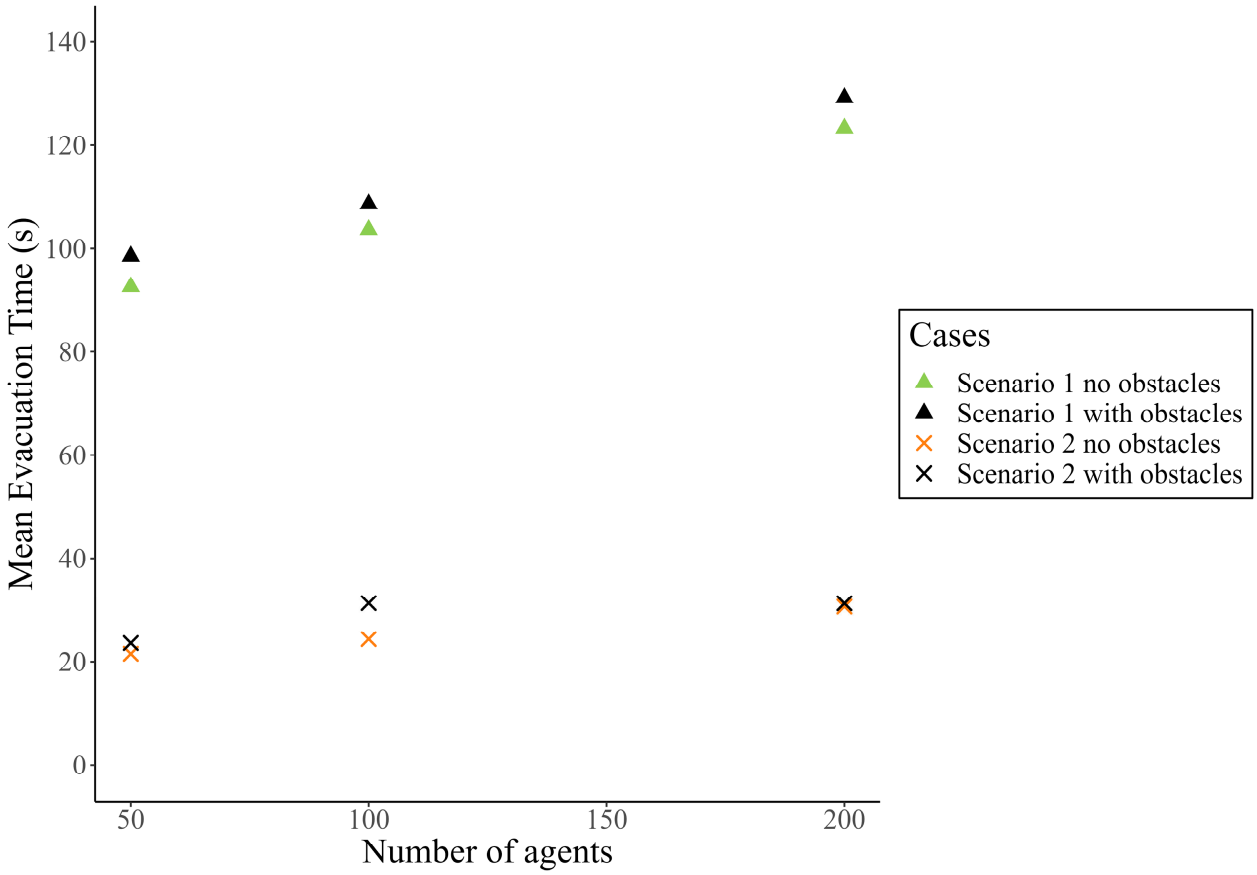

Figure 8. Mean evacuation times for Scenario 1 and Scenario 2 for cases with and without obstacles.

Table 4. Mean evacuation time for each crowd size and environments in Scenario 2.

Agents	No Obstacles	Obstacles	Difference
50	21.53	23.63	9.75%
100	24.40	31.43	28.83%
200	30.77	31.40	2.06%

4.2. Impact of the Tsunami Evacuation Stress

In the formulation of tsunami evacuation stress, which is described in Section 3.4, the sigmoid function's value depends solely on the distance from the current agents' position to the exit. Agents with equivalent distance values exhibit the same stress level, which is in accordance with Equations (5) and (6). This distance-dependent formulation yields most agents moving at desired velocities near to 2.77 m/s, evoking a running crowd in a high stress level, which is a very low-probability scenario. Despite the positive impact of tsunami stress on the mean evacuation time—agents take on average four times less time to evacuate—we may argue that in an actual evacuation, the stress level in a crowd certainly can vary among evacuees, with some individuals being in high stress and others in intermediate stress. To better understand the effect of mixed stress levels and subsequent spread, considering the internal susceptibility of agents in the crowd, the outcomes that were obtained are discussed below.

The mean evacuation time for the different crowd sizes for settings without and with obstacles plus a spread radius equals 2 m, is presented in (Figure 9). Compared to the results of Scenario 1 and Scenario 2, a similar trend is observed in terms of the number of agents in the simulation; the larger the crowd is, the longer the time it takes to evacuate 100% of pedestrians, with 49.73 s, 53.77 s, and 60.33 s for 50, 100, and 200 agents, respectively; for more details, see Table 5. With the inclusion of the tsunami stress propagation, the

mean evacuation time almost doubled compared to the values in the tsunami scenario (see Tables 4 and 5). This increment is reasonable, considering it as a trade-off between simulations with more realistic settings and simulations targeting the minimization of evacuation time.

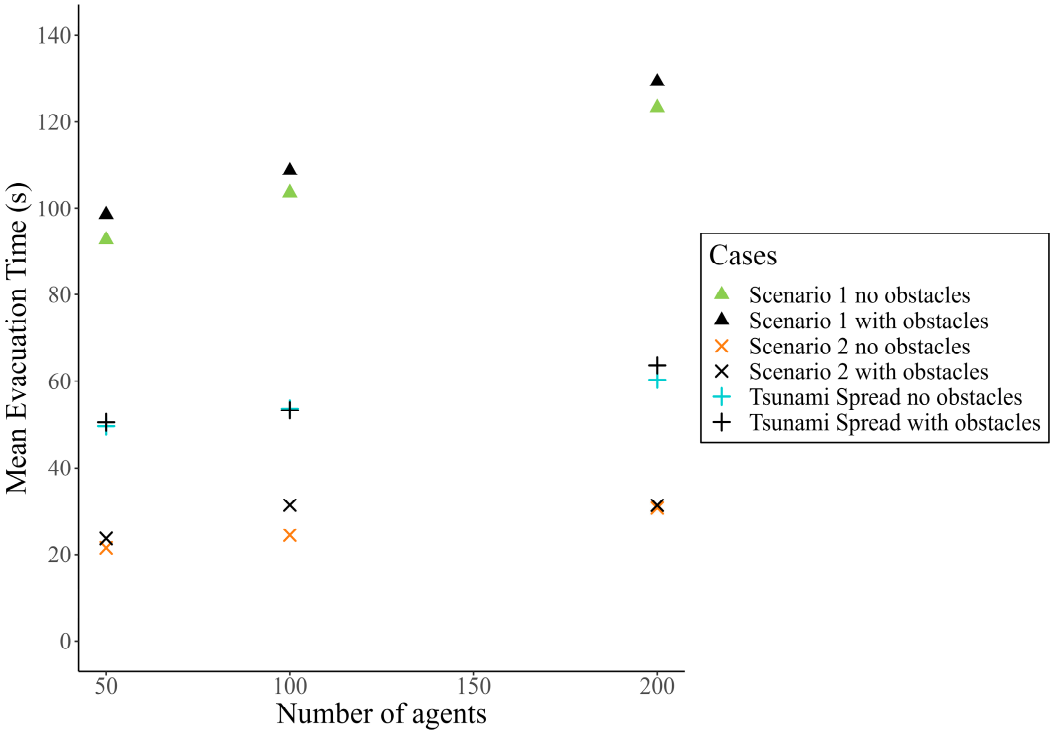

Figure 9. Mean evacuation time for each crowd size and environments, considering stress spread.

Table 5. Mean evacuation time for each crowd size and environments for the tsunami spread scenario.

Agents	No Obstacles	Obstacles	Difference
50	49.73	50.60	1.74%
100	53.77	53.37	−0.74%
200	60.33	63.70	5.58%

Furthermore, the same tendency is observed in terms of longer evacuation times and reduced impact due to the presence of obstacles; differences are less than 2% and 6% for 50 and 200 agents, respectively (see Table 5). For 100 agents, it takes slightly less time to evacuate settings with obstacles, with the difference being less than 1%.

Finally, in Figure 10, the mean crowdedness (agents' local density over time) is calculated based on the largest crowd. The crowdedness is not sensitive to spread radii between 0.5 m and 3 m. Overall, both environments show comparable patterns. When the simulation starts and agents are created, both curves increase steeply up to 5 s and continue growing up until 200 agents are reached. Because of obstacle avoidance and consequent manoeuvres, the instantaneous crowdedness remains below 0.45 ped/m^2 for environments with obstacles (black line). For cases without obstacles, the crowdedness is greater—approximately 0.56 ped/m^2, due to a higher concentration of agents. As a consequence of stress propagation, agents moving at comparable instantaneous velocities lead to the formation of groups, as depicted by cyan- and magenta-coloured lines in Figure 6. This clustering behaviour causes a sharp decrease at 30 s, when around 70% of agents have already evacuated. This drop continues until all agents in the simulation are evacuated and the crowdedness equals zero.

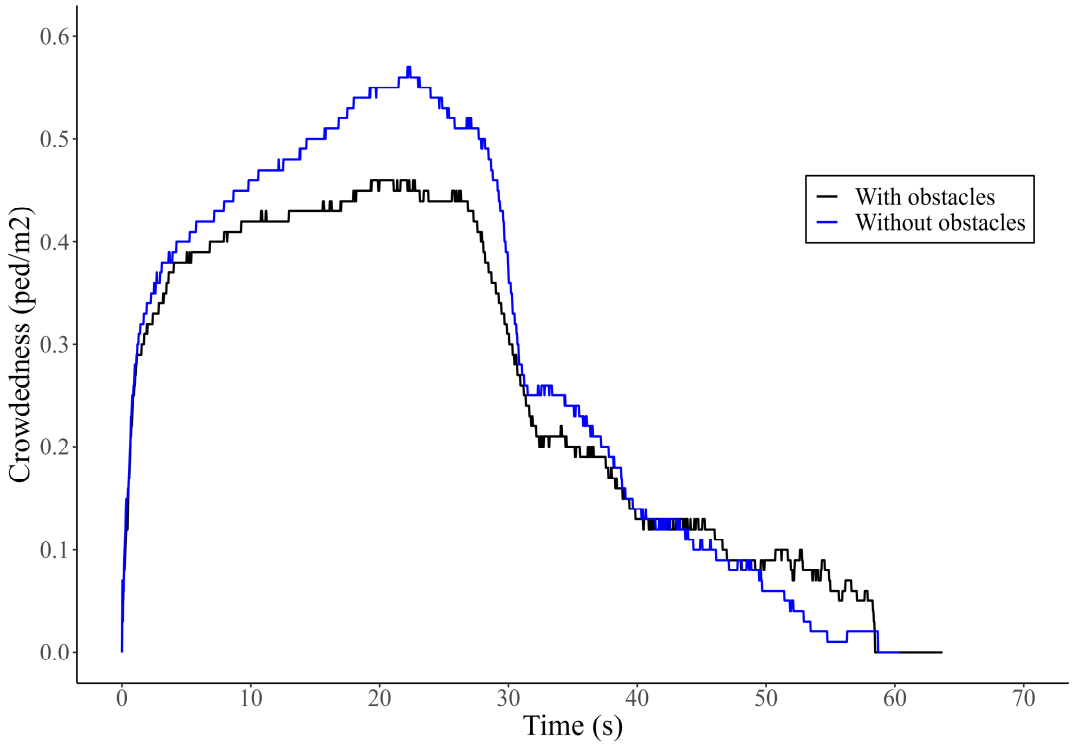

Figure 10. Mean crowdedness for 200 agents in the simulation considering environments with and without obstacles.

5. Discussion

To better understand the dynamics and verify whether the model can reproduce the macroscopic speed/density relationship in the cells adjacent to the exit, time windows for each scenario and crowd sizes are analysed. R-squared values are obtained to assess the capability of the model to replicate the linear relationship between the speed and density of agents. In this instance, the higher the density, the lower the mean speed, and vice versa. The emergent dynamics of our model are validated via the trend shown in Figure 11. The rest of the R-squared values are outlined in Table A1.

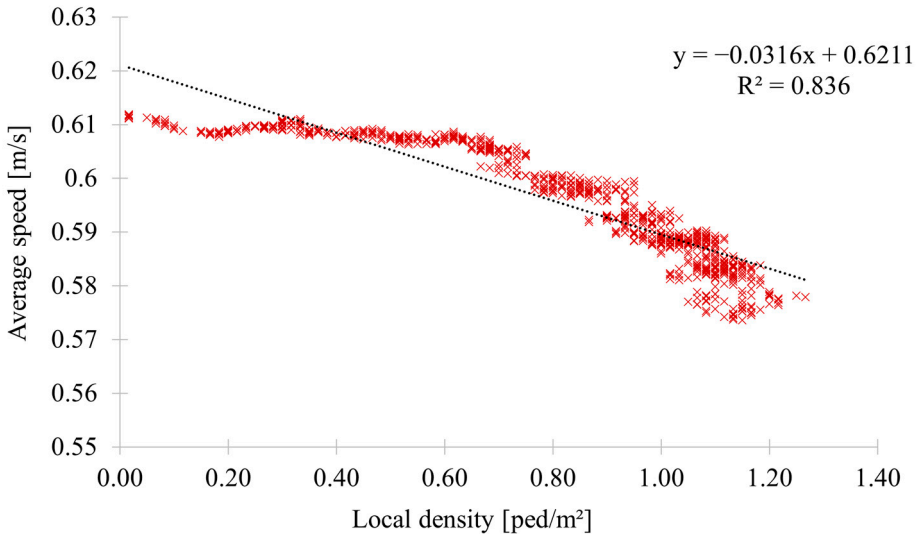

Figure 11. Linear regression between average speed and local density for crowds of 200 agents in Scenario 1, considering obstacles.

Even when the model can reproduce the speed/density relationship near the exit, to validate the simulation results, it is necessary to compare Scenario 1 against empirical data via a fundamental diagram. Yet, validation is more challenging for the hypothetical tsunami case (Scenario 2) due to data scarcity. Records from real tsunami evacuations are generally complicated to obtain. Because of ethical and safety reasons, these real-life emergencies are difficult to replicate under laboratory conditions. Even so, available CCTV records from governmental agencies or third parties are useful resources to obtain metrics. Through video processing techniques, pedestrian metrics (such as global and local density, instantaneous velocities, and trajectories) can help elucidate the complexities of human behaviour and the decision-making process in relation to tsunami evacuations.

6. Conclusions

In this study, a quantitative approach is proposed to estimate tsunami evacuation stress due to the occurrence of a near-field tsunami in central Chile. To represent pedestrian motion in ordinary situations but also in an evacuation context, the authors applied the social force model. Experimental scenarios are run in NetLogo for cases with and without a tsunami, utilising different desired velocity values. For the case of a tsunami, using a distance-dependent sigmoid function, the authors calculate tsunami stress for each agent. Three stress levels are defined: mild, intermediate, and high. Later, running values in the desired velocity, which are used to resemble individuals walking at a fast pace, are introduced. Simulation results show the positive impact on the mean evacuation time of implementing tsunami evacuation stress (Scenario 2). Agents take, on average, four times less time to evacuate compared to the case without a tsunami (Scenario 1). Nonetheless, one of the limitations of the approach is the limited stress variation among the crowd. In further simulations, to produce more realistic settings, a method to spread tsunami stress based on the internal susceptibility level of agents and the contagion rate should be presented. Due to the capability of agents to shift their stress levels from intermediate to high, and vice versa, the mean evacuation time nearly doubled when compared to the case with a tsunami. Still, the effect of spreading tsunami evacuation stress between evacuees is reasonable; the mean evacuation time is an intermediate value between Scenario 1 and Scenario 2. This result is considered a trade-off between simulations with more realism and simulations aiming at minimising the total evacuation time. Nevertheless, the outcomes of this research are valuable to advance the understanding of human behaviour in tsunami evacuations.

During a real tsunami scenario, it is not possible to predict a crowd's behaviour. However, the outcomes of this research are helpful for deepening our understanding of the benefits of including socio-psychological variables such as tsunami evacuation stress in computer models. Incorporating such variables in tsunami evacuation simulations is useful for improving current evacuation plans and preparedness in tsunami-prone cities. A better understanding of the complexities of human behaviour is necessary for sustainable evacuation. Therefore, this research contributes to SDG 11 Sustainable cities and communities by increasing disaster resilience.

For future works, to consider the effect of inundated cells in the simulations, a repulsive tsunami interactive force accounting for the willingness of pedestrians to move away from flooded areas would be helpful for representing the evacuation process more accurately. This enhancement of the social force model in a tsunami context would improve the realism of evacuations, contributing to sustainable evacuations and increasing disaster preparedness in coastal areas at risk to tsunamis. Moreover, city-wide evacuations can be investigated by enlarging the environment. The capability of agents to avoid obstacles successfully while maintaining their private space makes it possible to explore post-earthquake settings by analysing the debris on roads or sidewalks. Finally, in the context of global climate change, the need for multi-hazard and interdisciplinary approaches is becoming evident. This research has great potential to contribute to multi-hazard disaster preparedness.

Author Contributions: Conceptualisation, methodology, formal analysis, investigation, resources, data curation, writing—original draft preparation; C.F. and H.S.L.; writing—review and editing, C.F., H.S.L. and E.M.; software, C.F. and E.M.; visualisation, C.F.; supervision, H.S.L. and E.M.; project administration, funding acquisition, H.S.L. All authors have read and agreed to the published version of the manuscript.

Funding: This research received no external funding.

Institutional Review Board Statement: Not applicable.

Informed Consent Statement: Not applicable.

Data Availability Statement: Data are contained within this article.

Acknowledgments: Figure 2 was created in Lucid (lucid.co). The NetLogo model is used for tsunami evacuation modelling and will be available in the first author's GitHub repository profile (https://github.com/Kontysita/Tsu_evac_via_SFM.git). The first author is supported by the JICA SDGs Global Leadership program.

Conflicts of Interest: The authors declare no conflicts of interest.

Appendix A

The values in Table A1 are acceptable. For instance, in Scenario 1, crowds of 50 agents navigating environments without obstacles have an R-squared value of 90%. Similarly, crowds of 100 and 200 individuals, evacuating in settings with obstacles, present values of 79% and 84%, respectively. In the case with a tsunami (Scenario 2), higher R-squared values are obtained for settings without obstacles: crowds of 50 and 100 agents have values of 85% and 77%, respectively, while crowds of 200 agents reached an R-squared value of 91%, but only a 59% value for environments with obstacles.

Table A1. Speed/density R-squared values for both scenarios and environments.

Scenario	Agents	Time Frame (s)	No Obstacles	Obstacles
Scenario 1	50	66.50–78.13	89.59%	
	50	65.93–77.53		57.16%
	100	66.66–87.83	76.24%	
	100	65.37–82.30		79.24%
	200	66.20–99.80	63.80%	
	200	65.83–92.87		83.60%
Scenario 2	50	16.83–19.10	84.53%	
	50	16.76–19.63		81.19%
	100	16.90–20.43	77.36%	
	100	16.83–21.43		69.99%
	200	16.70–19.20	90.84%	
	200	16.80–21.77		58.86%

References

1. ElDesconcierto.cl. Available online: https://www.eldesconcierto.cl/nacional/2019/10/27/multitudinaria-marcha-que-une-vina-y-valparaiso-se-dirige-al-congreso.html (accessed on 28 April 2022).
2. Reuters. Available online: https://www.reuters.com/graphics/SOUTHKOREA-STAMPEDE/CHRONOLOGY/zjvqjqmmlpx/index.html (accessed on 30 January 2023).
3. Cornes, F.E.; Frank, G.A.; Dorso, C.O. Fear propagation and the evacuation dynamics. *Simul. Model. Pract. Theory* **2019**, *95*, 112–133. [CrossRef]
4. Cao, R.F.; Lee, E.W.M.; Yuen, A.C.Y.; Chan, Q.N.; Xie, W.; Shi, M.; Yeoh, G.H. Development of an evacuation model considering the impact of stress variation on evacuees under fire emergency. *Saf. Sci.* **2021**, *138*, 105232. [CrossRef]
5. Cimellaro, G.P.; Ozzello, F.; Vallero, A.; Mahin, S.; Shao, B. Simulating earthquake evacuation using human behavior models. *Earthq. Eng. Struct. Dyn.* **2017**, *46*, 985–1002. [CrossRef]
6. Mao, Y.; Yang, S.; Li, Z.; Li, Z. Personality trait and group emotion contagion based crowd simulation for emergency evacuation. *Multimed. Tools Appl.* **2020**, *79*, 3077–3104. [CrossRef]

7. Takabatake, T.; Fujisawa, K.; Esteban, M.; Shibayama, T. Simulated effectiveness of a car evacuation from a tsunami. *Int. J. Disaster Risk Reduct.* **2020**, *47*, 101532. [CrossRef]
8. Helbing, D.; Farkas, I.; Vicsek, T. Simulating dynamical features of scape panic. *Nature* **2000**, *407*, 487–490. [CrossRef]
9. Chen, X.; Treiber, M.; Kanagaraj, V.; Li, H. Social force models for pedestrian traffic–state of the art. *Transp. Rev.* **2018**, *38*, 625–653. [CrossRef]
10. Wilensky, U.; Rand, W. *An Introduction to Agent-Based Modelling: Modelling Natural, Social, and Engineered Complex Systems with Netlogo*; The MIT Press: Cambridge, MA, USA, 2015; pp. 29–40.
11. Mas, E.; Suppasri, A.; Imamura, F.; Koshimura, S. Agent-based Simulation of the 2011 Great East Japan Earthquake/Tsunami Evacuation: An Integrated Model of Tsunami Inundation and Evacuation. *J. Nat. Disaster Sci.* **2012**, *34*, 41–57. [CrossRef]
12. Solís, I.A.; Gazmuri, P. Evaluation of the risk and the evacuation policy in the case of a tsunami in the city of Iquique, Chile. *Nat. Hazards* **2017**, *88*, 503–532. [CrossRef]
13. Lee, H.S.; Sambuaga, R.D.; Flores, C. Effects of Tsunami Shelters in Pandeglang, Banten, Indonesia, Based on Agent-Based Modelling: A Case Study of the 2018 Anak Krakatoa Volcanic Tsunami. *J. Mar. Sci. Eng.* **2022**, *10*, 1055. [CrossRef]
14. Helbing, D.; Molnár, P. Social force model for pedestrian dynamics. *Phys. Rev. E* **1995**, *51*, 4282–4286. [CrossRef] [PubMed]
15. Helbing, D.; Farkas, I.J.; Molnar, P.; Vicsek, T. Simulation of pedestrian crowds in normal and evacuation situations. In *Pedestrian and Evacuation Dynamics*; Schreckenberg, M., Sharma, S.D., Eds.; Springer: Berlin, Germany, 2002; pp. 21–58.
16. Helbing, D.; Buzna, L.; Johansson, A.; Werner, T. Self-Organised Pedestrian Crowd Dynamics: Experiments, simulations, and Design Solutions. *Transp. Sci.* **2005**, *39*, 1–24. [CrossRef]
17. Siyam, N.; Alqaryouti, O.; Abdallah, S. Research Issues in Agent-Based Simulation for Pedestrians Evacuation. *IEEE Access* **2020**, *8*, 134435–134455. [CrossRef]
18. Sahal, F.L.; Péroche, M. Complementary methods to plan pedestrian evacuation of the French Riviera's beaches in case of tsunami threat: Graph- and multiagent-based modelling. *Nat. Hazards Earth Syst. Sci.* **2013**, *13*, 1735–1743. [CrossRef]
19. Callejas, E.; Inostrosa-Psijas, A.; Moreno, F.; Oyarzun, M.; Carvajal-Schiaffino, R. COVID-19 Transmission During a Tsunami Evacuation in a Lockdown City. In Proceedings of the 39th International Conference of the Chilean Computer Science Society (SCCC), Coquimbo, Chile, 16–20 November 2020; pp. 1–8.
20. Astudillo, G.; Gil-Costa, V.; Marin, M. Efficient simulation of natural hazard evacuation for seacoast cities. *Int. J. Disaster Risk Reduct.* **2022**, *81*, 103300. [CrossRef]
21. León, J.; Castro, S.; Mokrani, C.; Gubler, A. Tsunami evacuation analysis in the urban built environment: A multiscale perspective through two modelling approaches in Viña del Mar, Chile, Coast. *Eng. J.* **2020**, *62*, 389–404. [CrossRef]
22. León, J.; Catalán, P.A.; Gubler, A. Assessment of Top-Down Design of Tsunami Evacuation Strategies Based on Drill and Modelled Data. *Front. Earth Sci.* **2021**, *9*, 744193. [CrossRef]
23. León, J.; March, A. Urban morphology as a tool for supporting tsunami rapid resilience: A case study of Talcahuano, Chile. *Habitat Int.* **2015**, *43*, 250–262. [CrossRef]
24. Flores, C.; Lee, H.S.; Mas, E.; Salar, J. Tsunami evacuation in a massive crowd event using an agent-based model. In Proceedings of the 37th Conference on Coastal Engineering, Sydney, Australia, 4–9 December 2022. [CrossRef]
25. Lomnitz, C. Major Earthquakes of Chile: A Historical Survey, 1535–1960. *Seismol. Res. Lett.* **2004**, *75*, 368–378. [CrossRef]
26. Madariaga, R.; Métois, M.; Vigny, C.; Campos, J. Central Chile Finally, Breaks. *Science* **2010**, *328*, 181–182. [CrossRef]
27. CSN. National Seismological Centre University of Chile. Available online: https://www.sismologia.cl/informacion/grandes-terremotos.html (accessed on 27 February 2022).
28. Carvajal, M.; Cisternas, M.; Catalán, P.A. Source of the 1730 Chilean earthquake from historical records: Implications for the future tsunami hazard on the coast of Metropolitan Chile. *J. Geophys. Res. Solid Earth* **2017**, *122*, 3648–3660. [CrossRef]
29. Gorrini, A.; Crociani, L.; Vizzari, G.; Bandini, S. Stress estimation in pedestrian crowds: Experimental data and simulations results. *Web Intell.* **2019**, *17*, 85–99. [CrossRef]
30. Challenger, W.; Clegg, W.C.; Robinson, A.M. *Understanding Crowd Behaviours: Guidance and Lessons Identified*; UK Cabinet Office: London, UK, 2009; pp. 11–13.
31. Johansson, A.; Helbing, D.; Shukla, P.K. Specification of the social force pedestrian model by evolutionary adjustment to video tracking data. *Adv. Complex Syst.* **2007**, *10*, 271–288. [CrossRef]
32. Bassoli, E.; Vincenzi, L. Parameter Calibration of a Social Force Model for the Crowd-Induced Vibrations of Footbridges. *Front. Built Environ.* **2021**, *7*, 656799. [CrossRef]
33. Sticco, I.M.; Frank, G.A.; Dorso, C.O. Social Force Model parameter testing and optimisation using a high stress real-life situation. *Phys. A Stat. Mech. Appl.* **2021**, *561*, 125299. [CrossRef]
34. Chraibi, M. Oscillating behavior within the social force model. *arXiv* **2014**, arXiv:1412.1133.
35. Kretz, T. On Oscillations in the Social Force Model. *Phys. A Stat. Mech. Appl.* **2015**, *438*, 272–285. [CrossRef]
36. Wang, P.; Wang, X. Social Force in Pedestrian Crowd. *arXiv* **2021**, arXiv:2109.12597.
37. Wilensky, U. *NetLogo*; Center for Connected Learning and Computer-Based Modelling, Northwestern University: Evanston, IL, USA, 1999.
38. Mas, E.; Koshimura, S.; Imamura, F.; Suppasri, A.; Muhari, A.; Adriano, B. Recent Advances in Agent-Based Tsunami Evacuation Simulations: Case Studies in Indonesia, Thailand, Japan and Peru. *Pure Appl. Geophys.* **2015**, *172*, 3409–3424. [CrossRef]

39. Mas, E.; Adriano, B.; Koshimura, S. An Integrated Simulation of Tsunami Hazard and Human Evacuation in La Punta, Peru. *J. Disaster Res.* **2013**, *8*, 285–295. [CrossRef]
40. Wood, N.J.; Schmidtlein, M.C. Community variations in population exposure to near-field tsunami hazards as a function of pedestrian travel time to safety. *Nat. Hazards* **2013**, *65*, 1603–1628. [CrossRef]
41. Fraser, S.A.; Wood, N.J.; Johnston, D.M.; Leonard, G.S.; Greening, P.D.; Rossetto, T. Variable population exposure and distributed travel speeds in least-cost tsunami evacuation modelling. *Nat. Hazards Earth Syst. Sci.* **2014**, *14*, 2975–2991. [CrossRef]
42. Haghani, M.; Cristiani, E.; Bode, N.W.F.; Boltes, M.; Corbetta, A. Panic, Irrationality, and Herding: Three Ambiguous Terms in Crowd Dynamics Research. *J. Adv. Transp.* **2019**, *2019*, 58. [CrossRef]
43. YouTube. Available online: https://www.youtube.com/watch?v=HG1NkBo18uc&ab_channel=ClaudioFredesOsses (accessed on 28 February 2023).
44. Castellucci, H.I.; Viviani, C.A.; Molenbroek, J.F.M.; Arezes, P.M.; Martínez, M.; Aparici, V.; Bragança, S. Anthropometric characteristics of Chilean workers for ergonomic and design purposes. *Ergonomics* **2019**, *62*, 459–474. [CrossRef] [PubMed]
45. Chen, X.; Wang, J. An Entropy-Based Combined Behavior Model for Crowd Evacuation. *Entropy* **2022**, *24*, 1479. [CrossRef] [PubMed]
46. Moussaïd, M.; Helbing, D.; Theraulaz, G. How simple rules determine pedestrian behavior and crowd disasters. *Proc. Natl. Acad. Sci. USA* **2011**, *108*, 6884–6888. [CrossRef]
47. Johansson, A.; Helbing, D.; Al-Abideen, H.Z.; Al-Bosta, S. From crowd dynamics to crowd safety: A video-based analysis. *Adv. Complex Syst.* **2008**, *11*, 497–527. [CrossRef]
48. Tsurushima, A. Tunnel Vision Hypothesis: Cognitive Factor Affecting Crowd Evacuation Decisions. *SN Comput. Sci.* **2022**, *3*, 332. [CrossRef]